

ISSN: 1672 - 6553

JOURNAL OF DYNAMICS AND CONTROL

VOLUME 9 ISSUE 2: 1 - 10

PERFORMANCE COMPARISON OF
LQR AND LESO-BASED CONTROL
STRATEGIES FOR ROBUST DC
MOTOR REGULATION

Haneesh K. M¹, Jisha P², Prajoona
Valsalan³

¹Department of Electrical and Electronics
Engineering, CHRIST University, Bangalore

²Department of Electronics and Communication
Engineering, BMS College of Engineering,
Bangalore

³College of Engineering Dhofar University
Salalah, Oman

PERFORMANCE COMPARISON OF LQR AND LESO-BASED CONTROL STRATEGIES FOR ROBUST DC MOTOR REGULATION

Haneesh K. M¹, Jisha P², Prajoona Valsalan³

¹Department of Electrical and Electronics Engineering, CHRIST University, Bangalore

²Department of Electronics and Communication Engineering, BMS College of Engineering, Bangalore

³College of Engineering Dhofar University Salalah, Oman

¹haneesh.km@christuniversity.in ²jjishap.ece@bmsce.ac.in, ³pvalsalan@du.edu.om

Abstract: This study evaluates two modern control strategies applied to Separately Excited DC Motors (SEDCM) to achieve robust speed regulation. The performance of SEDCM in applications like automation and robotics is usually affected by internal or external disturbances. The Linear Quadratic Regulator (LQR) strategy uses a cost-minimal algorithm to generate state feedback to obtain optimal tracking. Linear Extended State Observer (LESO) is a robust control strategy that estimates system states and disturbances and applies for real-time compensation. The performance of these two control strategies employed on an SEDCM was evaluated for tracking performance, and disturbance rejection. This study also analyzed the impact of LESO gain values for pole placement. Proper selection of gain values ensures faster response, lower overshoot, and stability. The results show that both the control strategies ensure the desired tracking performance but LESO shows superior performance both in time response and in disturbance rejection, which will make LESO suitable for many similar applications.

Keywords: Disturbance Rejection, Linear Extended State Observer, LQR, Optimal Control, Robust Control, SEDCM.

1. Introduction

DC motors are preferred for industrial and research applications as they offer precise speed control and high starting torque. SEDCMs are used in automation, robotics, and machine tools due to their control simplicity. In linear system control of SEDCM generally, PID controllers are effective and offer flexibility through tuning gain coefficients. Even though PID controllers provide effective control, they are prone to internal or external disturbances in complex systems [1]. PID controllers are not suitable for nonlinear time-varying and multi-variable systems. State-feedback, robust or adaptive control techniques are preferred for such systems. Model Predictive Control (MPC) is a technique suggested for complex nonlinear systems, in which the system behavior is predicted based on a system model and optimized over a specific period. Even though MPC offers fast response and optimal performance, it requires significant computing resources to ensure quick response in multi-variable systems with constraints [2]. LQR is an optimal control technique in which a quadratic cost function is minimized by balancing system performance and control input. The state feedback is calculated based on the system model to ensure performance and stability. The LQR technique is used in many applications that aim for precision control [3]. LQR control was reported to improve settling time and overshoot over traditional PID controllers [4].

Active Disturbance Rejection Control (ADRC) uses state estimation using a model and continuously compensates for parameter variations and disturbances in real-time. LESO is an ADRC technique that gained popularity recently in various industrial applications. LESO offers robust performance without depending on an accurate model for prediction [5]. This attribute helps to ensure robust system performance when the system parameters vary or variations are not known accurately. Studies show that the LESO improves the control effectiveness under various uncertainties [6, 7]. LQR and LESO strategies find applications in contemporary industrial applications as they offer superior performance under uncertainties. The optimal control law used in LQR helps in achieving desired

performance while applying to multivariable systems whereas LESO offers resilience against model inaccuracies and uncertainties with precise estimation abilities. Both these control techniques are finding applications in both research and industrial settings in the quest for low-cost and energy strategies to obtain desired performance and resilience under uncertainties and parameter variations [8, 9].

This paper investigates the potential of LESO in ADRC strategies and contrasts it with the traditional LQR approach. The main contributions of this work include the design and implementation of LESO for online disturbance estimation and rejection, a systematic comparison of LESO and LQR using simulation studies, and frequency response analysis to assess robustness and stability under uncertainties. This study aims to provide insights into the advantages and limitations of LQR and LESO control strategies, guiding the selection of appropriate control methods for DC motor applications in complex industrial settings.

2. System Modelling

SEDCMs are finding applications in robotics, industrial automation, electric traction, and machine tools due to their precise speed control capability and higher starting torque generation. Even though AC motors are dominant in industrial applications now, SEDCMs are still relevant and used for many small and medium power applications. Developing a mathematical model is mandatory for analyzing the performance and designing controllers for complex dynamic systems.

2.1 Mathematical Modeling of the SEDCM

The dynamics of an SEDCM can be described by the following differential equations [10].

Electrical Dynamics is given by $V_a(t) = L_a \frac{di_a(t)}{dt} + R_a i_a(t) + e_b(t)$, where $V_a(t)$ is the armature voltage (V), L_a is the armature inductance (H), R_a is the armature resistance (Ω), $i_a(t)$ is the armature current (A) and $e_b(t)$ back emf (V)

Mechanical Dynamics is represented by $J \frac{d\omega(t)}{dt} + B\omega(t) = T_m(t)$, where J is the rotor inertia ($\text{kg}\cdot\text{m}^2$), B the viscous friction coefficient ($\text{N}\cdot\text{m}\cdot\text{s}/\text{rad}$), $\omega(t)$ the Angular velocity (rad/s), and $T_m(t)$ Motor torque ($\text{N}\cdot\text{m}$)

The back EMF and motor torque are related to the angular velocity and armature current, respectively $e_b(t) = K_e \omega(t)$ and $T_m(t) = K_t i_a(t)$, where K_e and K_t are the back EMF constant and torque constant, respectively.

2.2 State-Space Representation

Considering the state variables of the system as $x_1(t) = i_a(t)$ Armature current, $x_2(t) = \omega(t)$ Angular velocity [11]

The state-space model is formulated as

$$\begin{aligned} \dot{x}(t) &= Ax(t) + Bu(t) \\ y(t) &= Cx(t) \end{aligned}$$

where $x(t) = \begin{bmatrix} x_1(t) \\ x_2(t) \end{bmatrix}$, $u(t) = V_a(t)$, $y(t) = \omega(t)$

The matrices A , B , and C are defined as

$$A = \begin{bmatrix} -\frac{R_a}{L_a} & -\frac{K_e}{L_a} \\ \frac{K_t}{J} & -\frac{B}{J} \end{bmatrix}, \quad B = \begin{bmatrix} 1 \\ L_a \\ 0 \end{bmatrix}, \quad C = [0 \quad 1]$$

3. Linear Quadratic Regulator (LQR) Design

The LQR is designed to minimize the cost function $J = \int_0^\infty (x(t)^T Q x(t) + u(t)^T R u(t)) dt$

where Q and R are weighting matrices that balance state deviations and control effort [12]

For this system, the weighting matrices are chosen as $Q = \begin{bmatrix} q_1 & 0 \\ 0 & q_2 \end{bmatrix}$, $R = r$.

The optimal control law is $u(t) = -Kx(t)$, where K is the gain matrix computed by solving the Algebraic Riccati Equation (ARE) $A^T P + PA - PBR^{-1}B^T P + Q = 0$, The gain matrix K is then $K = R^{-1}B^T P$

4. Active Disturbance Rejection Control

A robust controller should reject internal and external disturbances to ensure desired performances under uncertainties. ADRC technique is implemented to do so using a state estimation method. The extended state observer will estimate the system states and disturbances in real-time. This LESO-based approach enables real-time estimation and compensation of disturbances, enhancing the robustness and performance of the DC motor control system. [13, 14]

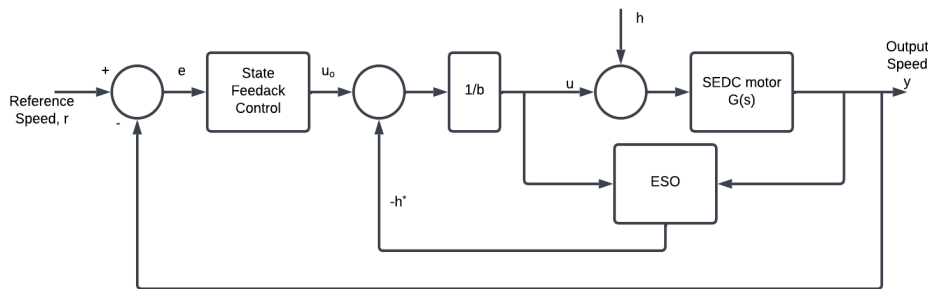


Figure 1. Schematic diagram of LESO

The dynamic behavior of a SEDCM is represented by the transfer function connecting motor speed $\omega(s)$ to the armature voltage $V_a(s)$ and load torque $T_d(s)$.

$$\omega(s) = G_m(s)V_a(s) + G_d(s)T_d(s)$$

Here, $G_m(s)$ represents the transfer function from armature voltage to motor speed, and $G_d(s)$ denotes the transfer function from load torque to motor speed. Assuming a nominal constant load torque, the system can be approximated by a second-order transfer function

$$\omega(s) = \frac{b}{s^2 + a_1 s + a_0} V_a(s) - T_d(s)$$

In the time domain, this corresponds to the differential equation $\dot{y} = -a_1 y - a_0 y + bu$, where y represents the motor speed, u is the control input (armature voltage), and a_0 , a_1 , and b are system parameters. The term $h(y, u, d) = -a_1 y - a_0 y$ encapsulates the generalized disturbance, encompassing internal dynamics and external perturbations.

To facilitate control design, we define an augmented state vector $z = [z_1, z_2, z_3]^T$, where $z_1 = y$ (motor speed) $z_2 = \dot{y}$ (acceleration), $z_3 = h(y, u, d)$ (generalized disturbance), Assuming h is differentiable, the state-space representation becomes $\dot{z} = Az + Bu + Eh$

$$\text{with matrices } A = \begin{bmatrix} 0 & 1 & 0 \\ 0 & 0 & 1 \\ 0 & 0 & 0 \end{bmatrix}, \quad B = \begin{bmatrix} 0 \\ b \\ 0 \end{bmatrix}, \quad E = \begin{bmatrix} 0 \\ 0 \\ 1 \end{bmatrix}$$

and output equation $y = Cx$

To estimate the states, including the generalized disturbance, a LESO is designed as $\dot{\hat{z}} = A\hat{z} + Bu + L(y - \hat{y})$, where \hat{z} is the estimated state vector, L is the observer gain matrix, and $\hat{y} = C\hat{z}$ is the estimated output. The observer gain L is chosen to ensure the stability and desired performance of the observer.

The observer vector L is selected in such a way that all the poles of the observer are located at the desired pole location $-\omega_o$. This pole placement will ensure the desired performance and stability. The characteristic polynomial for the observer is [7]

$$\lambda = (s + \omega_o)^3 = s^3 + 3\omega_o s^2 + 3\omega_o^2 s + \omega_o^3$$

This polynomial defines the desired eigenvalues for the observer system matrix $A - LC$, ensuring that all poles are located at $-\omega_o$.

The gain of the observer L is calculated using the pole placement method. The eigenvalues of the matrix $A - LC$ is determined to locate the poles [10]. The poles of the observer are placed at $-\omega_o$, the LESO is designed to have accurate state estimation and fast convergence. If the location of poles is far from the origin, it will ensure a quick response but at the same time they will amplify noises, similarly, poles closer to the origin can make the response sluggish, this demands a trade-off while selecting the pole position [15].

5. Simulation Setup

The state space model for the SEDCM described in section 3 was used to simulate the control strategies. The parameters used for the SEDCM are given in Table 1. For the LQR simulation weighing matrices R and Q were selected as 0.01 and $\text{diag}(100, 8)$ respectively. The weighing matrix Q values were picked to emphasize control of armature velocity and armature current respectively. The value of R is selected to penalize the large control input. The simulations were done on MATLAB R2023a on a standard PC setup. LQR simulations were done for 5 seconds so the responses, angular velocity, and armature current reached their steady-state value. LESO simulations were done by taking internal disturbances as an additional state. The poles of the observer were placed with a gain factor of a_0 and with a bandwidth of $\omega_o = 20$. To analyze the effect of the gain factor on LESO performance, the gain factors were varied from 0 to 100. The frequency response of the systems is analyzed by finding the bode plot of the system under various gain scaling factors.

Table 1. Parameter values

Parameter	Value
DC Motor Parameters	
R_a (Armature Resistance)	1 Ω
L_a (Armature Inductance)	0.5 H
K_t (Torque Constant)	0.01 Nm/A
K_e (Back EMF Constant)	0.01 V/(rad/s)
J (Moment of Inertia)	0.01 kg·m ²
B (Viscous Friction)	0.001 Nm/(rad/s)
LQR Parameters	
State Weighting Matrix (Q)	diag([100, 8])
Control Effort Weighting (R)	0.01
LESO Parameters	
Observer Gain Scaling Factors (a_0)	[0, 0.1, 1, 10, 100]
Observer Bandwidth (ω_o)	20

6. Results and Discussions

The simulation results show that the LQR and LESO control offer good tracking performance under normal conditions, but when disturbances are considered, LESO outperforms LQR. Fig 2 shows the speed response of SEDCM with LQR control. Using the trial-and-error method, R and Q values were selected as 0.01 and diag (100, 8) respectively. The system with LQR shows precise tracking with a lower settling time, also the control effort needed to maintain the speed was found to be low. The system performance with the LQR is shown in Fig. 4. A step disturbance of magnitude 0.5 is applied at $t = 5$ s, and the angular velocity response is sluggish and shows steady-state error.

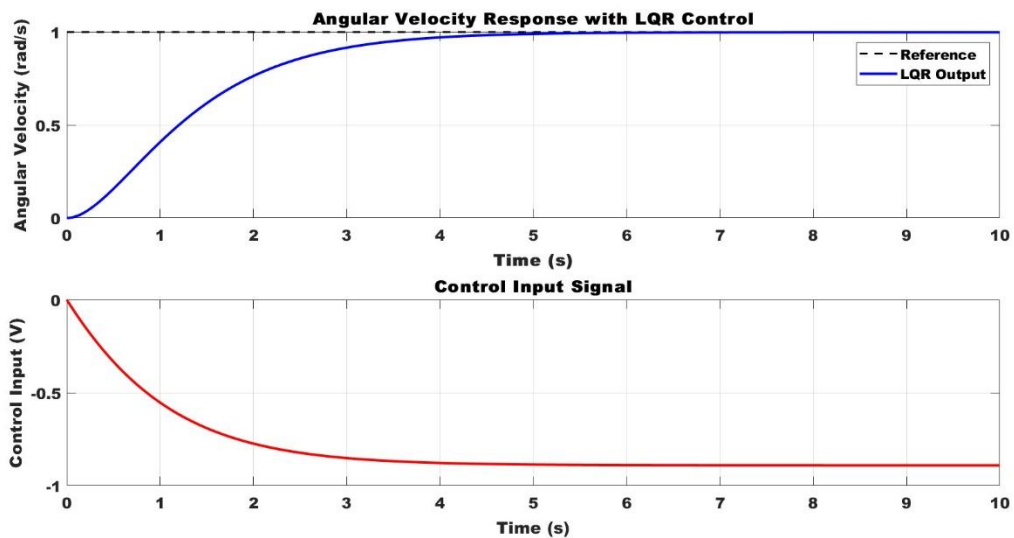


Fig. 2 Tracking performance of the system with LQR control

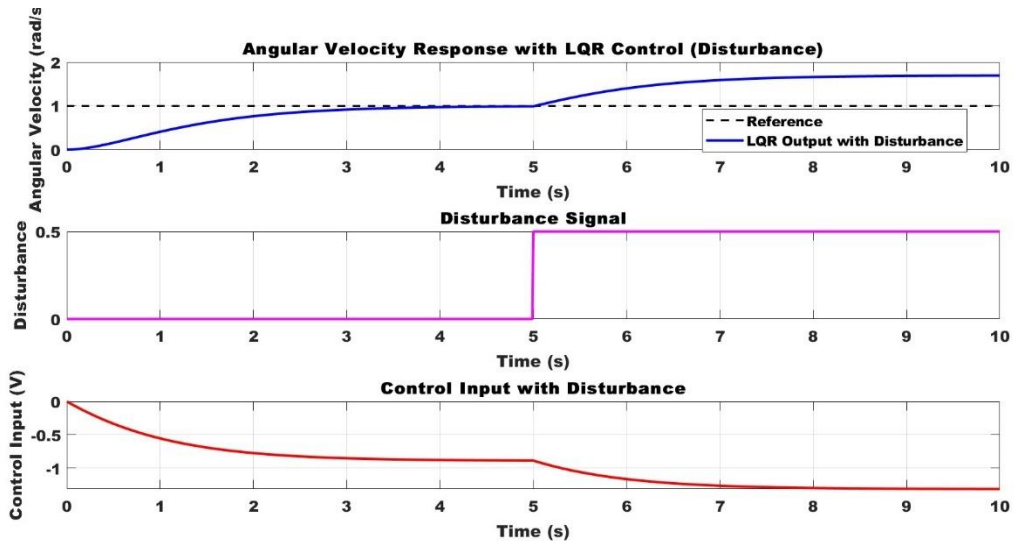


Fig. 3 Performance of the LQR system under disturbance

The time response of LESO implemented on the SEDCM is shown in Fig. 4. The results show excellent tracking performance for angular velocity and armature current. The performance is evaluated with a change in speed introduced from $t=2.5$ s. The results also show that the tracking response is unaffected by the introduction of disturbance.

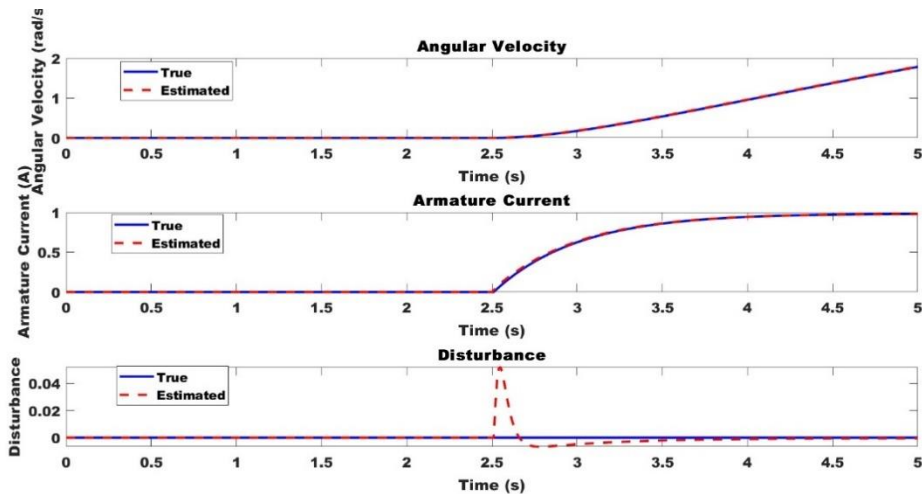


Fig. 4 Tracking performance of LESO

In the simulation, the gain scaling factor of LESO was selected as 10. Since the performance of the controller depends on the gain value, the time response of the system with LESO was studied for various gain scaling factors ($a_0 = 0, 0.1, 1, 10, 100$). The response with variations in gain values is shown in Fig. 5. From the results, it can be seen that a gain value of 10 gives the best performance for settling time and overshooting. At lower values of a_0 system response is sluggish and shows poor disturbance rejection, at higher values of a_0 the response is generally faster but overshoot increases.

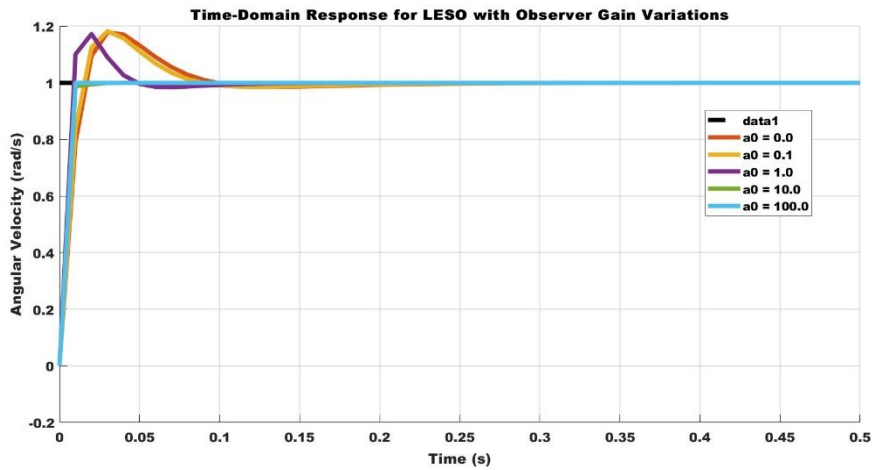


Fig 5. Time response of the system with LESO gain variations

To analyze the system performance with the LESO controller, Gaussian noise is added to the output and simulated. The response is given in Fig. 6 and it shows that the motor angular velocity is tracking the reference precisely even under added noise.

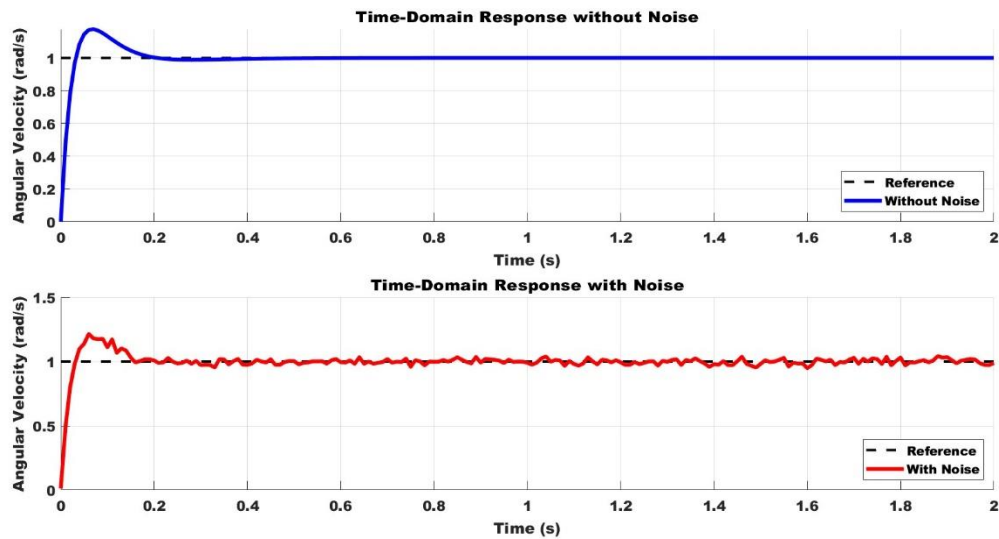


Fig. 6 Performance of the system with LESO under disturbance

Bode plots for different a_0 configurations reveal the system's frequency response and robustness to varying gain settings (Fig. 7). Systems with higher a_0 values demonstrate enhanced bandwidth and faster disturbance rejection, evidenced by greater phase margins and reduced low-frequency gain. These characteristics confirm that the LESO effectively attenuates low-frequency disturbances while maintaining stability across a wide frequency range. Conversely, lower a_0 values restrict the observer's bandwidth, leading to limited disturbance rejection and slower dynamics.

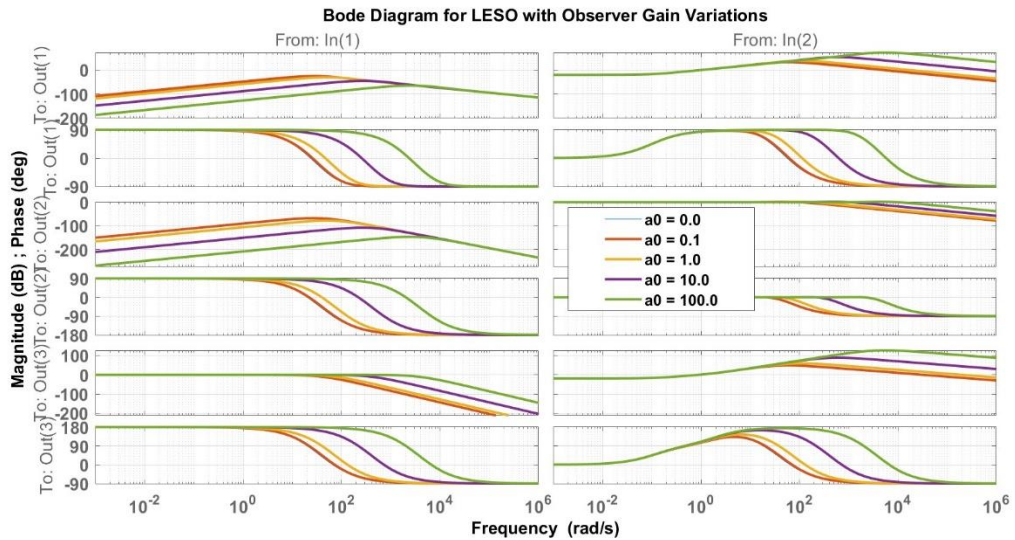


Fig 7. Bode plot of the LESO under gain variations

The Nyquist plot reveals that the LESO system is stable for all input-output mappings. Input 1 (control input u) effectively regulates Output 1 (angular velocity), maintaining stability with no encirclements of the critical $-1 + j0$ point as shown in Fig. 8. Input 2 (measurement error) impacts disturbance estimation, with the elliptical plot for Output 3 (generalized disturbance) showing robust handling of uncertainties. The low-frequency response indicates good tracking performance, while the high-frequency loops highlight effective noise rejection but expose sensitivity trade-offs. The LESO demonstrates robust disturbance rejection and state estimation, decoupling disturbance effects from control. These results validate LESO's superior performance to traditional controllers under uncertain conditions.

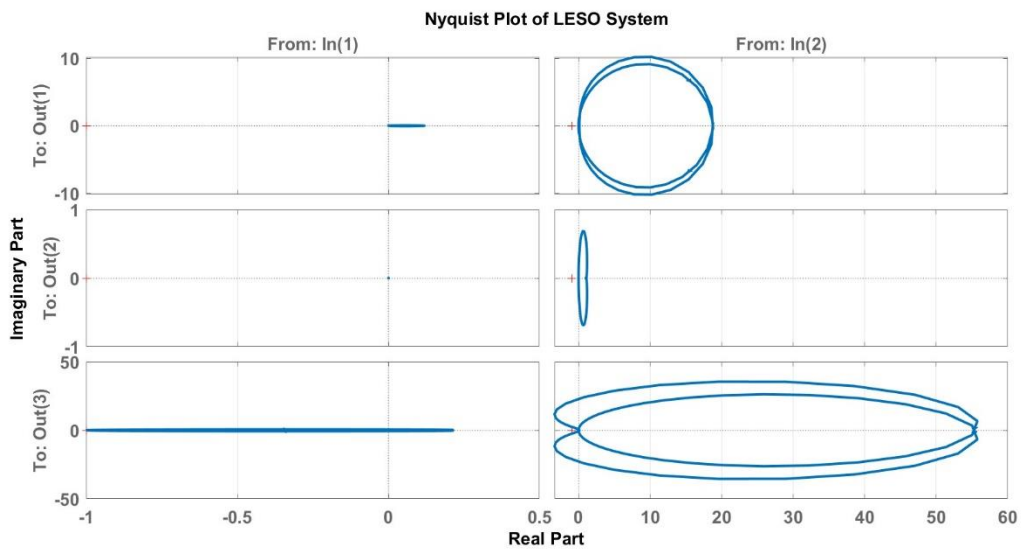


Fig. 8. Nyquist Plot for the system with LESO

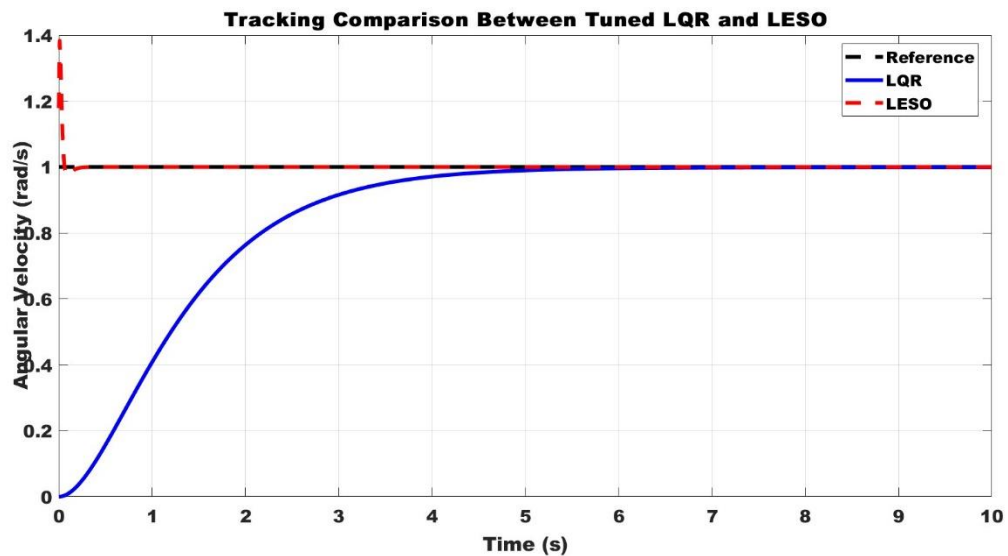


Fig 9. Performance comparison of LQR and LESO

The LQR controller offers optimal control but is susceptible to internal or external source disturbances. Motor operations generally create heating and may trigger changes in parameter values, also the torque and temperature variations can affect the performance of the LQR controller, as it uses a state feedback method. On the other hand, LESO uses an estimation technique and subsequent corrections, the systems with LESO offer robust performance even under disturbances.

7. Conclusion

Control of SEDCM using two modern control strategies was evaluated in this study. A state space model for the system was developed and LQR and LESO controllers were implemented and simulated on the MATLAB platform to evaluate their performances. The LQR control was found to ensure optimal performance in terms of tracking and stability. Even though LQR was offering excellent tracking performance, the time response of LQR was found to depend on the tuning of R and Q matrices. The LESO implementation was done with a gain value $L = 10$, but the impact of variation in gain values was analysed in detail to fix the value of L. The frequency analysis of the LESO controller was also studied to analyse the stability of the system under various gain values. It was found that the system is showing good resilience even with gain variations. The disturbance rejection capabilities of the LESO system were studied by adding noise to the system and found to be tracking very well even under disturbances. From the study, it was concluded that LESO is a robust control strategy for systems similar to SEDCM with internal and external disturbances.

References

- [1] Freitas, J.B.S., Marquezan, L., de Oliveira Evald, P.J.D. et al. A fuzzy-based Predictive PID for DC motor speed control. *Int. J. Dynam. Control* 12, 2511–2521 (2024). <https://doi.org/10.1007/s40435-023-01368-2>
- [2] Wang, Ning, Xiaojie Qiu, Changqing Long, Jun Chen, and Wenchao Meng. "Gaussain Process-based MPC for DC Motor Servo System with State Constraints and Load Disturbance." In *2024 7th International Symposium on Autonomous Systems (ISAS)*, pp. 1-6. IEEE, 2024.

- [3] S. Dani, D. Sonawane, D. Ingole and S. Patil, "Performance evaluation of PID, LQR and MPC for DC motor speed control," 2017 2nd International Conference for Convergence in Technology (I2CT), Mumbai, India, 2017, pp. 348-354, doi: 10.1109/I2CT.2017.8226149.
- [4] D. Ivanova and N. Valov, "LQR-based PID Control of DC Motor Speed," 2024 9th International Conference on Energy Efficiency and Agricultural Engineering (EE&AE), Ruse, Bulgaria, 2024, pp. 1-5, doi: 10.1109/EEAE60309.2024.10600621
- [5] J. Linares-Flores et al., "Sliding Mode Control Based on Linear Extended State Observer for DC-to-DC Buck–Boost Power Converter System With Mismatched Disturbances," in *IEEE Transactions on Industry Applications*, vol. 58, no. 1, pp. 940-950, Jan.-Feb. 2022, doi: 10.1109/TIA.2021.3130017.
- [6] Bagua, H. (2023). Performance Comparison of PID and LQR Control for DC Motor Speed Regulation. *The Journal of Engineering and Exact Sciences*, 9(12), 19429. <https://doi.org/10.18540/jcecvl9iss12pp19429>
- [7] Okoro IS, Enwerem CO. Robust control of a DC motor. *Heliyon*. 2020 Dec 19;6(12):e05777. doi: 10.1016/j.heliyon.2020.e05777. PMID: 33376824; PMCID: PMC7758373.
- [8] J. Humaidi, Amjad, and Ibraheem Kasim Ibraheem. 2019. "Speed Control of Permanent Magnet DC Motor with Friction and Measurement Noise Using Novel Nonlinear Extended State Observer-Based Anti-Disturbance Control" *Energies* 12, no. 9: 1651. <https://doi.org/10.3390/en12091651>
- [9] Bharti, J., Phadke, G., Patil, D. (2020). Optimization of DC Motor Speed Control Using LQR Technique. In: Kumar, A., Paprzycki, M., Gunjan, V. (eds) *ICDSMLA 2019. Lecture Notes in Electrical Engineering*, vol 601. Springer, Singapore. https://doi.org/10.1007/978-981-15-1420-3_157
- [10] M. B. Aremu, M. Abdel-Nasser, N. M. Alyazidi and a. S. El-Ferik, "Disturbance Observer-Based Bio-Inspired LQR Optimization for DC Motor Speed Control," in *IEEE Access*, vol. 12, pp. 152418-152429, 2024, doi: 10.1109/ACCESS.2024.3478362.
- [11] J. Humaidi, Amjad, and Ibraheem Kasim Ibraheem. 2019. "Speed Control of Permanent Magnet DC Motor with Friction and Measurement Noise Using Novel Nonlinear Extended State Observer-Based Anti-Disturbance Control" *Energies* 12, no. 9: 1651. <https://doi.org/10.3390/en12091651>
- [12] H. Yin, L. Cao, X. Zeng, K. H. Loo and C. Sun, "Fast Dynamic Control of Dual-Active-Bridge DC–DC Converter Based on an Adaptive Linear Extended State Observer," in *IEEE Transactions on Power Electronics*, vol. 39, no. 12, pp. 16019-16030, Dec. 2024, doi: 10.1109/TPEL.2024.3454209.
- [13] Z. Xia, X. Yu, X. Wu and Y. Dou, "An Enhanced Linear Extended State Observer-based Sensorless IPMSM Drives with Robustness Against Current Measurement Offset Error," in *IEEE Transactions on Transportation Electrification*, doi: 10.1109/TTE.2024.3443809.
- [14] Z. Hu, S. Shen, Y. Su and Z. Li, "Dc Motor Control: A Global Prescribed Performance Control Strategy Based on Extended State Observer," 2024 36th Chinese Control and Decision Conference (CCDC), Xi'an, China, 2024, pp. 3490-3495, doi: 10.1109/CCDC62350.2024.10587568.
- [15] Zhang, Z., Chen, Y., Feng, X. et al. Linear active disturbance rejection speed control with variable gain load torque sliding mode observer for IPMSMs. *J. Power Electron.* 22, 1290–1301 (2022). <https://doi.org/10.1007/s43236-022-00429-7>